

RAM

● ROBOTICS
AND
MECHATRONICS

REALIZATION OF TIME-DOMAIN PASSIVITY CONTROL FOR
ROBOTIC VARIABLE IMPEDANCE TELEOPERATIONSYSTEMS:
THEORY AND EXPERIMENTAL DEMONSTRATION

M. (Myrthe) Weisbeek

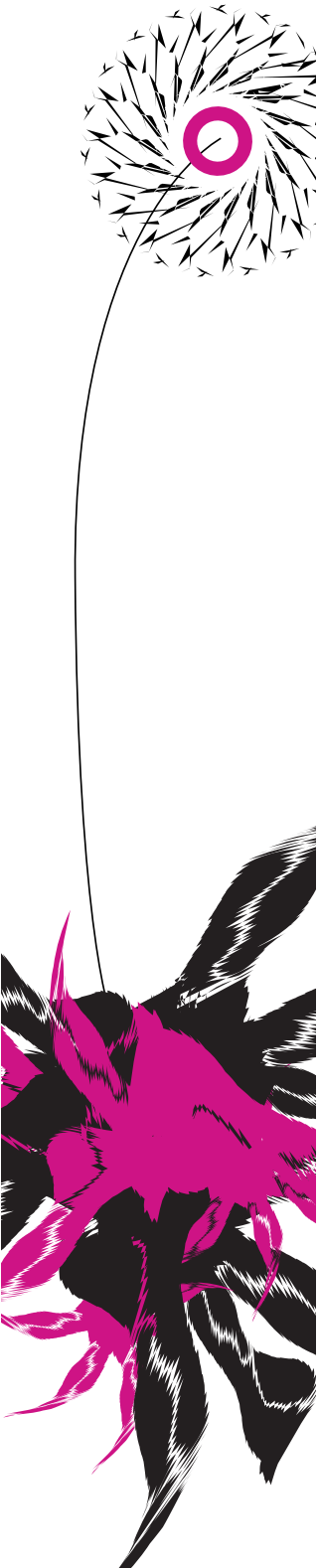
MSC ASSIGNMENT

Committee:

dr. ir. D. Dresscher
dr. ir. R.G.K.M. Aarts

January, 2025

002RaM2025
Robotics and Mechatronics
EEMCS
University of Twente
P.O. Box 217
7500 AE Enschede
The Netherlands



Preface

This thesis was written as part of my graduation project for the master programme Systems and Control at the University of Twente. I conducted the project at the Robotics and Mechatronics (RaM) research group within the i-Botics open innovation centre relating to tele-robotics. I experienced RaM as a very professional research group consisting of a lot of friendly people invested in helping each other out. My supervisor for this project, Dr. Ir. Douwe Dresscher, was very helpful and understanding throughout the graduation project, which I appreciated a lot. The project itself was very interesting. Passivity- and Energy Tank-based control was often only touched upon as a minor subject in many of my courses. This had stoked my curiosity, and I am glad I got to dive deeper into the subject matter. Albeit not without hiccups, the combined theoretical and practical aspects of my graduation project made it a very educational and satisfying project. Thank you to everyone involved for the enjoyable time I had at RaM.

Myrthe Weisbeek, January 2025, Enschede

Abstract

Time Domain Passivity Control (TDPC) is a form of control that aims to guarantee a system to behave passively. Previous literature has developed a 'Two-Layer Architecture' (TLA) for Bilateral Tele-robotic systems combining passivity and transparency control objectives by combining TDPC and Impedance Control using energy tanks and energy exchange protocols. Literature has demonstrated that variable impedance (VI) control enables superior transparency performance in typical applications for Tele-robotics. However, literature has shown that combining variable impedance with TLA is non-trivial and thus an extension of TLA was proposed to solve issues that arise due to this combination. Literature demonstrates validity of this solution under highly limited circumstances, in simulation of a Bilateral Tele-Robotic setup consisting of two robot arms. In this thesis, the proposed extension is investigated when measurement noise is present throughout the system. The effect measurement noise has on the extension turn out to be non-trivial under certain circumstances. Therefore, the noise characteristics of applications must always be considered when aiming to combine TLA with VI control lest passivity and transparency guarantees may not be satisfactory. The exact circumstances and resulting consequences in which measurement noise affects TLA with VI are presented in this thesis.

Contents

CHAPTER 1 INTRODUCTION	8
1.1 INTRODUCTION	8
1.2 RELATED WORK	8
1.3 RESEARCH GOAL	9
1.4 METHOD	10
1.5 REPORT OUTLINE	11
CHAPTER 2 BACKGROUND THEORY	12
2.1 PASSIVITY.....	12
2.2 TIME-DOMAIN PASSIVITY CONTROL	12
2.3 IMPEDANCE MODULATION	14
2.4 VARIABLE IMPEDANCE MONITORING (VIM)	15
2.5 DISCRETE PASSIVITY TANK BEHAVIOUR	15
2.6 DISCRETE TIME STATISTICS	15
CHAPTER 3 ANALYSIS.....	18
3.1 RELEVANT REALIZATION FACTORS	18
3.2 MAGNITUDE OF BOOKKEEPING INACCURACY	21
3.3 SIGNIFICANCE OF INACCURACY	21
3.4 HYPOTHESES.....	22
CHAPTER 4 SETUP & DESIGN	24
4.1 MATERIALS	24
4.2 SYSTEM DESIGN & IMPLEMENTATION.....	24
4.3 EXPERIMENT DESIGN.....	25
CHAPTER 5 RESULTS.....	29
5.1 VALIDATION	29
5.2 VERIFICATION - RELEVANT REALIZATION FACTORS	32
5.3 VERIFICATION - MAGNITUDE OF BOOKKEEPING INACCURACY	33
CHAPTER 6 DISCUSSION	36
6.1 – VALIDATION.....	36
6.2 – RELEVANT REALIZATION FACTORS	37
6.3 – MAGNITUDE OF BOOKKEEPING ACCURACY	37
6.4 – SIGNIFICANCE OF INACCURACY.....	37
CHAPTER 7 CONCLUSION	39
7.1 – RELEVANT REALIZATION FACTORS	39
7.2 - MAGNITUDE OF BOOKKEEPING ACCURACY	39
7.3 - SIGNIFICANCE OF INACCURACY	39
7.4 – LIMITATIONS & IMPROVEMENTS.....	39
7.5 – CONSEQUENCES	40
7.6 – FUTURE RESEARCH.....	40
7.7 – CONCLUSION	40
BIBLIOGRAPHY.....	41

List of Figures

Name	Description	Section
F11-1	Rudimentary schematic of bi-lateral tele-operation setup	1.1
F21-1	Bondgraph representation of a 2 port system	2.1
F22-1	Extended illustration of a two layer architecture	2.2
F411-1	Validation results of passivity layer in simulation	5.1
F411-2	Validation results of passivity layer in physical setup	5.1
F412-1	Validation results of VIM in simulation	5.1
F412-2	Validation results of VIM in physical setup	5.1
F413-3	Noise measurements of physical setup	5.1
F42-1	Verification results of varying noise with non-constant position trajectory	5.2
F43-1	Verification results of varying noise for constant position	5.3
F43-2	Verification results of varying noise for constant position, observed energies	5.3

List of Tables

Name	Description	Section
33-1	Constant parameters for all experiments	4.3
331-1	Validation constant parameters	4.3
331-2	Validation experiments	4.3
332-1	H1 verification constant parameters	4.3
332-2	H1 verification experiments	4.3
333-1	H2 verification constant parameters	4.3
333-2	H2 verification experiments	4.3
T413-1	Noise measurement of physical setup	5.1.3
T43-1	Experiment data when varying position, correlation, and noise	5.3

List of Equations

Equation	Description	(sub)section
1	Passivity condition	2.1
2	Single port passivity condition	2.1
3		
4	Energy Tank update rule	2.2
5	Single port Energy Tank update rule	2.2
6	Impedance Control Law	2.3
7	Continuous time potential energy change of a constant stiffness spring	2.3
8	Two Port Passivity condition	2.3
9	Two Port Energy Tank update rule for variable impedance	2.4
10	Two Port Energy Tank prediction at time N.	2.5
11.1	Mean value of discrete signal	2.6.1
11.2	Auto-Covariance of discrete signal	2.6.1
11.3	Cross-Covariance of discrete signal	2.6.1
12	Cross-Covariance for three discrete signals with zero mean	2.6.2
13.1	Extension of equations 11 and 12 with an approximation error	2.6.3
13.2	Reformulation of 13.1 when multiplied by N	2.6.3
14.1	Local formulation of the energy tank update rule with communication delay and noise	3.1.1
14.2	Remote formulation of the energy tank update rule with communication delay and noise	3.1.1
15	Energy tank update rule with only noise for either side	3.1.2
16	Repeat of equation 10	3.1.2
17	Combination and Reformulation of the Energy Tank prediction at time N substituting the noisy Energy tank update rule	3.1.2
18	Reformulation of equation 17	3.1.2
19	Reformulation of equation 18 using stochastic quantity descriptions	3.1.2
20	Generic form of equation 19 at time N for uncorrelated noise	3.1.3
21	Generic form of equation 19 at time N for correlated noise	3.1.4
22	Potential Energy of impedance controller affected by noise	3.2

Abbreviations and symbols

Abbr. / Symbol	Description	Introducing (sub)section
VIM	Variable Impedance Monitoring	1.2.5
DoF	Degree of Freedom	1.4
MCI	Monte Carlo Integration	2.6
	Power	2.1
	Flow variable	2.1
	Effort variable	2.1
	Control effort	2.1
	Position error rate	2.1
	j-th energy observer	2.2
	Change of state in the state estimator	2.2
	Passivity control effort of the previous discrete timestep	2.2
	Mass coefficient	2.3
	Damping coefficient	2.3
	Spring coefficient	2.3
	Generic stochastic variables used only within this chapter	2.6
	Approximation error due to using MCI	2.6
	Covariance	2.6
	Mean	2.6
	Varying part due to e.g. noise of a signal	3.1
H	Energy tank energy	2.2
U	Potential energy	3.2

Chapter 1 Introduction

1.1 Introduction

Teleoperation systems are comprised of an unpredictable, local human operator and an unknown, remote environment, mediated through two spatially separated, communicating interfaces of which at least one is a robot. These systems are used or developed for use in a variety application fields, including surgical, construction, inspection, defence & security, and many other types of robotics fields [10, 14]. Although autonomous robots are also seen in these fields, full autonomous operation is often computationally demanding or insufficient to meet the full complexity required for typical tasks in these fields [11]. Teleoperation allows combining the benefits of robotics with the intelligence and complex skills of a human operator. Sometimes, both a human operator and an autonomous high-level algorithm, i.e. artificial intelligence, can be combined in various degrees [12].

In some fields such as surgical robotics a human operator is may benefit from haptic feedback [7, 9]. An example of a haptic robotics system is a bilateral teleoperation system composed of a robot at both interfaces of the system. Figure F11-1 illustrates a bilateral teleoperation system. This allows active reflection of the states and interactions of one robot to the other, from e.g. a remote to local robot. This reflection of states, such as the reflection of remote force to the local side, is experienced as haptic feedback. When reflection is possible in either direction, the system is bilateral [14].

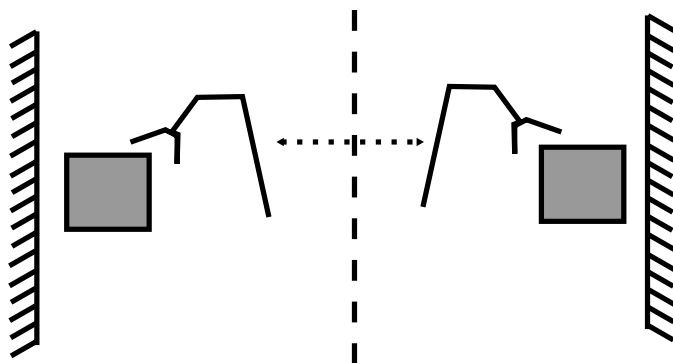


Figure F11-1 – *Bilateral teleoperation system. Left is the local side and right the remote side. Both sides have an environment, such as a wall (line with lines) and a mass (block). The arms are connected via a bidirectional communication system represented by the dotted arrow line.*

Bilateral teleoperation systems are powerful. They allow a human to extend their spatial limitations and abilities by allowing them to operate with for example enhanced strength, precision, or dexterity from a comfortable, safe distance. This may allow for higher quality of job performance while promoting safety where applicable. Therefore, research in this field can prove invaluable for society.

Extensive research has been conducted in bilateral teleoperation systems. Part of this research involves impedance modulation, a concept that is used to further enhance user experience and performance in bilateral teleoperation. This thesis will further investigate a key technique developed to combine impedance modulation with modern bilateral teleoperation techniques. It will specifically focus on systems that suffer from realization effects such as noise.

1.2 Related Work

Extensive work has been done in establishing a suitable architecture for bilateral telemanipulation systems. These systems need to be safe for the human and reliable in performance. Because both the local human operator and the remote environment are highly uncertain and unpredictable, classical stability- or performance-focussed or model-based control may no longer be feasible or sufficient to

guarantee stability and safety in teleoperation [15]. Instead, literature finds passivity and transparency are more useful qualities to pursue in teleoperation [1]. The exact details of literature relating to these two qualities will be discussed in 'Chapter 2 Background Theory'.

Concisely, in literature, typically two controllers are used in series: a Time Domain Passivity Controller (TDPC) for passivity and an Impedance Controller for transparency. To guarantee passivity and to minimally restrict transparency, which is both desirable, accurate energy bookkeeping is necessary. Here bookkeeping refers to keeping track of the potential energy in the impedance controller which is done via an energy tank. When the potential energy of the controller, based on its states, does not match the tracked energy in the tank, based on a series of measurements, the difference represents an inaccuracy. If the bookkeeping is too inaccurate, either passivity can no longer be guaranteed, or transparency of the system suffers [1, 3, 8].

A typical implementation of an impedance controller is that of a linear spring [2, 8]. The potential energy of the controller will change when its impedance (i.e. spring stiffness) is modulated. Impedance modulation can be desirable but the change in potential energy requires additional care in bookkeeping. This was remarked by the author of [8] who then also designed a method referred to in this thesis as 'Variable Impedance Monitoring' (VIM) to improve bookkeeping accuracy. The design and use of VIM was only a side effect of their research as their focus laid elsewhere. As a result, the sufficiency of VIM was not rigorously investigated.

VIM was derived mathematically by the author of [8] who showed in simulation that VIM ensures accurate energy bookkeeping for impedance modulation for a limited set of cases. Their conclusion was that a lack of VIM negatively impacted transparency and thus VIM was used for their other experiments. Further investigation of the effect of VIM was not done.

1.3 Research Goal

As impedance modulation is a desirable method with applications relevant to society, it is imperative that the theory surrounding its application is sound and complete. Following from the previous section, VIM must be investigated more thoroughly.

The goal of VIM is to ensure accurate bookkeeping by expanding the monitoring strategy for a constant-impedance controller so that the strategy remains valid for a modulated-impedance controller. Therefore, bookkeeping accuracy will be the leading metric in the investigation of VIM.

As was concluded, the theoretical application of VIM on idealized, as opposed to real, systems appears mathematically sound. However, there is a lack of experimental evidence for VIM accounting for realization effects. Realization effects are model and measurement noise, quantization, sampling time, and communication delay. This leaves open the question whether VIM can safely and satisfactorily be applied to real systems under all circumstances without undesirable effects caused by VIM directly.

These two insights lead to the formulation of the research goal of this thesis:

“Investigate the behaviour of Variable Impedance Monitoring and the resulting energy bookkeeping accuracy given a bilateral teleoperation system with a passivity and modulated-impedance controller which is under influence of realization effects”.

This research goal gives rise to several research questions that, once answered, will satisfy the research goal.

1.3.1 Relevant realization factors

The difference between the idealized systems for which VIM was designed and validated, and real systems for which VIM has not been validated yet, are realization factors. Realization factors such as noise may influence the behaviour of VIM and thus may lead to reduced bookkeeping accuracy.

RQ1 - “ Which realization factors affect bookkeeping accuracy ? ”

1.3.2 Magnitude of bookkeeping inaccuracy

Once the relevant realization factors have been identified, the question follows what circumstances affect the magnitude of the induced bookkeeping inaccuracy. This is important as it gives insights into when VIM may be reliably used.

RQ2 - “ Which circumstances or quantities affect the presence of inaccuracy inducing realization factors ? ”

1.3.3 Significance of inaccuracy

Knowing which circumstances, or rather quantities, affect the magnitude of bookkeeping inaccuracy, the final question must answer what magnitudes these quantities must range in for the resultant bookkeeping inaccuracy to become undesirable, causing reduced transparency or breaking passivity. This may be compared to a nominal teleoperation setup in a modern robotics lab.

RQ3 - “What order of magnitude must the inaccuracy-affecting quantities have for bookkeeping inaccuracy to have significantly noticeable effects on transparency or passivity?”

With these three questions answered, it will be knowable for exactly which real systems VIM is a sufficient method and where the application of VIM may have undesirable consequences. This will satisfy the research goal.

1.4 Method

The three research questions will be answered by experimentally verifying a set of hypotheses. These hypotheses are based on the mathematical investigation of VIM when influenced by realization effects, of which only noise will turn out to be relevant for this.

To start, the relevant background theory found in literature will be provided in sufficient detail. After which the novel analysis is performed, detailing the derivation for a set of mathematical predictions for the behaviour of VIM. This is done by extending mathematical description of VIM as given in literature with a noise component. A brief section will be dedicated to the other realization effects during the analysis but will not be investigated further than that. This derivation then forms the basis for the hypotheses.

The system that will be extended with VIM will consist of a control system and a pair of spatially separated, communicating robots as specified in the research goal. The robots will be fully actuated, six Degree of Freedom (DoF) robots. However, to isolate the experiments from side-effects, all experiment trajectories will entail only one DoF end-effector motion. The specified control system will control the end-effector motion.

To ensure the experiment results are solely a product of the controlled variables, a set of validation experiments will be performed to validate the implementation of the design. These experiments will be performed both in simulation and on the physical setup.

The hypotheses will be verified through experiments mostly in simulation. Namely, simulation allows for a convenient and controlled way to define and vary the realization affects. A subset of these experiments will be performed on a physical setup, however, to enhance validity of this research. To ensure all experiments are comparable, where relevant, the position and impedance trajectories will be kept consistent over the experiments. The bookkeeping accuracy will be evaluated by comparing the observations, i.e. the energy tank trajectory, with the actual potential energy of the controller.

The thesis will be concluded with a detailed analysis of the results and a conclusion with recommendations for future research and reflection on improvements of the study presented in this thesis.

1.5 Report Outline

The report consists of seven chapters, the current one being 'Chapter 1 Introduction'. Each chapter consists of several sections to separate the content logically, and optionally subsections to improve readability where needed.

'Chapter 2 Background Theory' delves into the relevant mathematical background theory needed to support the derivation in the chapter after.

'Chapter 3 Analysis' presents the derivations that will lay the mathematical basis for the hypotheses. The hypotheses make a prediction regarding the behaviour of the system when it is placed in various controlled conditions, in an attempt to answer the research questions. The hypotheses will be presented in a parallel structure to the research questions.

'Chapter 4 Setup & Design' will elaborate on the available hardware and software that was used for the experiments. It will then provide the exact details on how the software of the system was implemented so that it meets the conditions specified in the hypotheses, utilizing some of the background theory of Chapter 2. After this, the experiments needed to validate the implementation and the experiments required to verify the hypotheses will be laid out in detail, including a justification.

'Chapter 5 Results' will showcase the results of these experiments. It will first showcase the validation experiments and conclude that the given software implementation enables valid hypothesis verification experiments. Observations will be presented regarding the nominal noise characteristics found in the physical setup as well. Then, the results for the hypothesis verification experiments will be showcased.

'Chapter 6 Discussion' will analyse the results in parallel to the order in which the hypotheses were presented. First elaborating on what went as expected and then zooming in on any inconsistencies in prediction versus result.

'Chapter 7 Conclusion' concludes the thesis with a concise analysis of the work presented in the rest of this thesis. The findings of the discussion will be laid out in parallel to the research questions, which will be answered. The work of this thesis will be reflected upon and recommendations for study improvements, as well as for future research will be presented.

Chapter 2 Background Theory

This chapter will discuss the detailed mathematical theory relevant for this thesis, expanding on the concepts mentioned in ‘section 1.2 Related Work’ as well as introducing additional background concepts.

2.1 Passivity

A passive system contributes to the goal of safety and performance by a strict guarantee of stability and remains passive upon proper interconnection with another passive system [1]. Port Hamiltonian (PH) systems are an essential part of modern literature involving passivity in teleoperation as its underlying theory is commonly applied or extended [1, 2, 7, 15]. Such a Port Hamiltonian system is illustrated in figure Fig21-1. Such a system may store energy and exchanges energy through power ports with an environment.

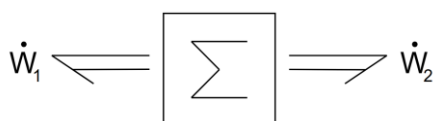


Fig21-1 - Bondgraph representation of some system with 2 power ports positive towards the environment.

The passivity condition applicable for such a system is given in equation (1). When the condition of equation (1) is met, it is said that the system behaves passive and thus provides stable dynamics. A (virtual) system may dissipate energy as well [5]. Dissipation will be neglected for this thesis, however, as it is not relevant for the research goal.

.....

The power through the i -th power port of the system is represented by \dot{W}_i with t the time. Integrating power yields a change of energy over the integration interval. Thus, equation (1) is a condition that states the total energy exchanged between a system and its environment must, at all instances of time t , result in positive semi-definite absorption of energy by the system. That is, the system is not allowed to cause a positive net-injection of energy into the environment.

A power port is represented by its conjugate variables (e, f) , i.e. a flow and an effort, and a direction [7, 15]. The conjugate variables can, for example, be a velocity and a force respectively. In particular, for an impedance controller with a single power port, the passivity condition is given by equation (2).

.....

This controller applies a control effort, e_c , to the interconnected environment, to control the dynamics of \dot{x} , some position error rate. An impedance controller, or in general an impedance-like system, dictates the behaviour of an effort variable while interconnected systems dictate the conjugate flow, i.e. an impedance controller has effort-out causality. From now on, this power port will be referred to as the control effort power port,

2.2 Time-Domain Passivity Control

Time-domain passivity control (TDPC) leverages the passivity condition. In [1] TDPC is implemented as a ‘passivity layer’ through an energy tank for energy bookkeeping, energy observers that use measurements to add or subtract energy from the energy tank, and a passivity controller. The observer

monitors energy flow through the power ports. Depending on the energy available in the tank, the passivity controller limits a desired effort coming from the ‘transparency layer’. The passivity controller outputs the resultant passivity effort that the complete control system is allowed to apply. The transparency layer houses some error controller which must be an impedance controller to be compatible with the architecture of [1]. The two layers, together with additional protocols to enhance performance, encompasses the complete architecture designed by [1].

The architecture as a block diagram with signals is illustrated in figure Fig22-1. It is illustrated in a more general form, however, with the inclusion of impedance modulation and generically mentioned state estimator and state predictor. The equations, where applicable, or pseudo code of each block is given below. All blocks except for the robot are defined in discrete time and only exist in discrete time.

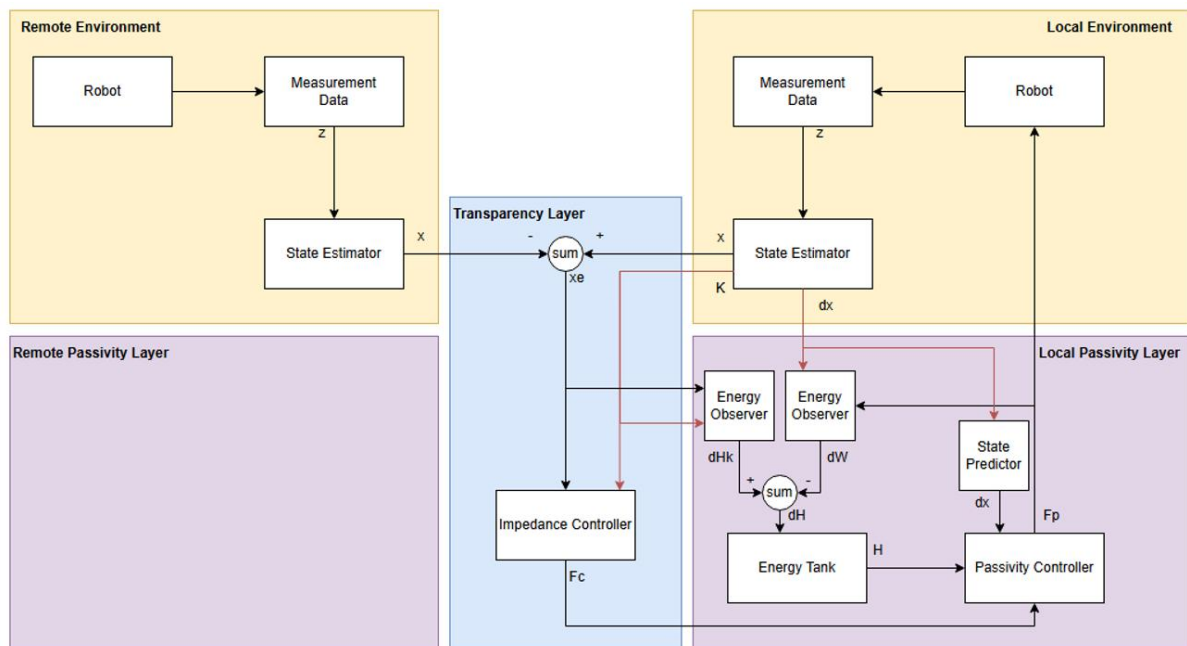


Fig22-1 – Block diagram of the Two-Layer architecture with notable extensions / generalizations. The blocks are grouped in different regions to indicate which blocks are part of the passivity and transparency layer, and which block belongs to neither. Some signals are coloured red to not confuse signals that cross each other. The labels for each signal are: z (measured data), x (estimated position state), K (estimated impedance state), dx (estimated / predicted change in position), dW (observed work done), dHk (observed energy change due to impedance modulation), dH (total energy change), H (energy tank level), x_e (position error between remote and local position estimate), F_c (desired control effort), F_p (limited / passivity control effort).

Robot – The continuous time system that responds to a discrete control action such as joint torques being applied. The system dynamics and environment interactions happen here. This is therefore not implemented by the architecture as it is the system that must be controlled.

Measurement Data & State Estimator – The measurement data represents a state such as the angle of the robot joints or the impedance based on an EMG signal. However, a measurement device has limitations in the precision and accuracy it can measure quantities with. An estimator must estimate the actual state from the noisy measurement data. A specific implementation is not provided by the architecture. Without a sufficient estimator, the state estimation signal may contain noise. Measurements are performed at a particular sampling frequency.

Impedance Controller – Based on the state estimates of both local and remote side, the controller determines a desired control effort. The details of this controller will be discussed later. The effort is sent to the passivity controller.

Energy Observer – The state estimates together with the force applied at the previous time-step are used by the observers to determine the energy through the controller power ports. This is the work done for a constant-impedance controller. For a modulated-impedance controller, the potential energy change due to impedance modulation is also observed from the state estimates.

Energy Tank – The observed energy changes are added or subtracted from the energy tank level. The update rule of the energy tank is given in equation (4). It is a discrete time equation defining the tank level difference equation for each time-step, .

.....

represents the i -th energy observer output. In case only a work done observer is considered, as in the paper of [1], the update rule becomes as equation (5).

.....

.....

Here, w_i comes from the state estimator and u_i is the passivity control output from the previous time-step.

Energy Exchange – This is not indicated in the block diagram as it will not be used in this thesis. However, the authors of [1] propose that the architecture allows tank energy to be exchanged between each side via a designable communication protocol. It is important that this protocol does not ‘generate’ energy, i.e. the energy added to one tank must not be more than the corresponding energy leaving the other tank.

State Predictor – The states for the next time-step must be predicted for use in the passivity controller. The architecture provides no directions for this either.

Passivity Controller – The desired (transparency) control effort together with the predicted states are used to predict the desired work done for the next time step. Using the energy tank level, the passivity controller computes:

1. Whether the desired work done will drain more energy from the tank than it has stored. In the case the desired work done is too large, the desired control effort is limited in the next step. Otherwise, the desired control effort is the output of the passivity controller.
2. In case the desired control effort must be limited, it computes the maximum allowed effort that will drain (part of) the tank. The specific protocol for this computation is free to be chosen.

2.3 Impedance Modulation

In [2] the transparency controller is described in more detail, formulated as an Intrinsically Passive Controller (IPC). It is established that this type of controller exhibits desirable performance and versatility in either position or force tracking, depending on how the parameters are chosen. The IPC behaves like a virtual mass-spring-damper system, described in equation (6). In continuous time, the IPC is a passive element. However, in discrete time, this is no longer guaranteed [8].

.....

The mass, m , damping, b , and spring, k , coefficients work on the controlled position error, e , and its time derivatives and can be as complex or simple as desired. In some literature, these coefficients are based on the robot kinematics and dynamics [3], while sometimes effective constants are derived empirically or learned [8, 3]. In tele-manipulation it was found to be effective to modulate the spring stiffness, or impedance, according to the impedance of the user's arm [8]. In this thesis, only the stiffness term will be non-zero.

With impedance modulation in mind, [2] introduces an additional power port for the spring component of the IPC. The power port can be used to model modulation of the impedance in a power continuous way. The power through this port is described in equation (7). This equation follows from the partial derivative of the energy of a linear spring, as derived in [2].

$$\dot{W}_s = \frac{\partial W_s}{\partial x} \dot{x} = kx\dot{x}$$

Consistently with the naming of \dot{W}_s , the impedance modulation power port will be named \dot{W}_m from now on.

The passivity condition of equation (2) can be extended with equation (7) so that both power ports of the modulated IPC are accounted for, yielding equation (8). The port \dot{W}_m is defined to positively head into the system.

$$\dot{W}_s + \dot{W}_m = \dot{W}_c$$

2.4 Variable Impedance Monitoring (VIM)

In [8] it was demonstrated that impedance modulation results in inaccurate energy bookkeeping when not accounting for the change in potential energy of the IPC. This is in-line with the findings of [2] regarding the inclusion of port \dot{W}_m . By including the energy observer of port \dot{W}_m in the energy tank update rule, [8] concluded that the energy bookkeeping is once again accurate. The technique of adding this energy observer to the update rule will be named Variable Impedance Monitoring (VIM) in this thesis. Now, the update rule with VIM is given in equation (9) which is comprised of equation (5) with the addition of equation (7) as was first done by the authors of [8].

$$\dot{W}_c + \dot{W}_m = \dot{W}_t$$

2.5 Discrete Passivity Tank Behaviour

In implementation, the updating of the passivity tank energy occurs in discrete time as it is updated each sample period when new measured data becomes available for the passivity observers and a new control effort is defined for the upcoming sample period. Using equation (9), the progression of the tank energy over each sample, up to the n -th sample, is given by equation (10). Equation (10) will be the equation used for the key derivations in the next section. It will be assumed that \dot{W}_m is zero.

$$W_t(n) = W_t(0) + \sum_{k=0}^{n-1} \dot{W}_c(k) \Delta t$$

2.6 Discrete time statistics

Part of the derivation in the next chapter will require knowledge of statistic quantity definitions for discrete time sampled stochastic variables. This will be covered in this section. Note that for simplicity of notation, the mathematical symbols used in this section have no relation to similar symbols used

..... — — —

It is trivial to verify that equation (eq20) also holds for one independent and two co-dependent stochastic variables such as ϵ_{1t} i.e. $\epsilon_{2t} = \alpha \epsilon_{1t} + \epsilon_{3t}$.

2.6.3 Approximation Error

So far it was neglected that MCI is an approximation with an approximation error. A fully correct approximation includes this error, as in equation (13.1).

..... —

Here, μ is some constant statistic quantity that describes one of the expectations, such as the mean or covariance. ϵ_{it} is its approximation with an unknown error-of-approximation term ϵ_{it} . Equation (13.1) clearly abides the LLN as when N approaches infinity, the error contribution converges to zero so that $\frac{1}{N} \sum \epsilon_{it} \rightarrow 0$.

If whatever signals ϵ_{it} describes have a small covariance and mean, relative to the mean of ϵ_{it} , then equation (13.2) is applicable. It shows that ϵ_{it} will always be a stochastic variable via the MCI approximation. Since the MCI approximation usually converges, it is assumed that ϵ_{it} has a zero mean and thus the sum over it remains bounded.

.....

Chapter 3 Analysis

In pursuit of answering the research question of this thesis, this chapter presents novel work that makes use of the presented background theory. In this chapter, the three research questions will be explored and analysed. The focus will lie on providing an exact formulation for each research question, and then an exact prediction where applicable. This chapter will finish by accumulating the findings into a set of hypotheses. These hypotheses should be verifiable such that the experiment results provide a sufficient answer to the research questions.

3.1 Relevant Realization factors

The first research question asks to investigate if and how realization factors may influence the port monitoring method, VIM. The following list of factors are relevant when considering realization effects: Noise; Communication delay; Discretization (continuous to discrete time); Sample time; Quantization. Each of these effects will be considered in this section. First, a description of VIM will be derived that includes these factors explicitly. Then, an exact prediction will be derived for the behaviour of VIM when it is subject to relevant realization factors.

3.1.1 Extended VIM formulation

In equations (14.1 and 14.2) of equation (10) has been reformulated to explicitly include noise and time delay. Considering communication delay, a separate equation may be formulated for each side. Which side a variable is defined for is indicated by a superscript with r for remote and l for local.

$$\begin{aligned} \dots & - \\ \dots & - \end{aligned}$$

Here, t represents the time instance at which data was send from one side to the other with a communication delay of τ . The variable n represents the noise component of the impedance measurement and p represents the noise component of the position measurement.

It is assumed the sampling time is constant and equal for both sides. If so, a sampling time would negate any effect of communication delay as communication from one side will arrive before the next sampling period. This causes τ for equations (14.1 and 14.2). Conversely, τ will not introduce any different behaviour to equations (14.1 and 14.2), but it will affect the number of samples N that fit within a timespan T . This may be relevant for later.

Finally, quantization affects the precision with which i and v can be measured. This may discretize any probabilistic descriptions of the noise on these signals and will affect the noise characteristics.

3.1.2 Stochastic noise

Temporarily excluding communication delay by defining $\tau = 0$ will simplify equations (14.1 and 14.2) to equation (15).

$$\dots -$$

The behaviour of equation (15) becomes apparent when summed over all time instances, as shown in equation (16). This sum represents the accumulated energy observed at only the port r .

$$\dots$$

In the derivation the assumption that σ is constant will be made, as this should sufficiently approximate the results of [8] where σ behaves like a series of step functions, making σ sparsely non-zero. With this assumption, the measure impedance change, ΔZ , each time-step, will reduce to only the noise change, ΔZ_{noise} .

Now, equation (15) can be expanded into equation (17). For the coming few equations, the time index will be omitted for brevity, until equation (20). Furthermore, index-sums over matrices will be used to compactly display the equations.

$$\dots -$$

It is helpful to separate ΔZ into further components. This results in equation (18).

$$\dots -$$

$$-$$

$$\dots - \dots$$

Consider equation (16) again. In the case the noise variables are stochastic variables, each time instance, t , of the signals represents a sample of the stochastic variables σ . A sum over these samples can be interpreted as something similar to the MCI approximation of the expectation covered last chapter, if the assumption is made that each stochastic variable has a zero mean. A zero mean assumption is a common assumption to make for typical measurement noise and will therefore be the only type of noise considered in this thesis [5]. Then, equation (16) can be reformulated in terms of probabilistic quantities.

It is unwieldy to try to predict the behaviour of VIM for every possible σ trajectory. Therefore, it will be assumed that σ is constant as this should allow for sufficient investigation of the research questions for the purpose of this thesis. Combining the MCI approximation with equations (16 and 18) yields equation (19).

$$\dots -$$

$$\dots -$$

$$\dots -$$

Here, μ represents the mean and Σ the (cross-)covariance consistent with the notation of section 2.6 on discrete time statistics. It may yield a more accurate prediction to truncate equation (19) of 'higher order' covariance terms, the terms over three signals σ , as the derivation of σ in 'Chapter 2 Background Theory' may not be entirely accurate. This form of equation (19) will be referred to as the 'truncated' form.

Now, two cases can be considered: The case in which some or all of the noise signals are correlated, and the case in which none are correlated.

3.1.3 Uncorrelated noise

With exactly zero correlation between the signals, equation (19) is simplified to equation (20) by using the definition of equation (13). Note that time indices will be included in the equations again, and that now σ is no longer time dependent as it is assumed constant.

$$\dots - \dots - \dots$$

To elaborate, each σ and σ of equation (19) are approximations of σ and σ respectively with some error ϵ as covered last chapter. When the error-free mean is zero and there is no correlation between signals, these errors remain. The errors, ϵ , that remain are stochastic variables. As mentioned in ‘Chapter 2 Background Theory’, these sums over N will likely remain bounded and cause σ to behave like a stochastic variable. This means that uncorrelated noise will affect the behaviour of VIM. The equation also shows that a larger position error σ will scale parts σ and thus will scale its variance.

3.1.4 Correlated noise

In the case that the noise signals are correlated, equation (19) can be evaluated further to equation (21). To elaborate, it is similar to equation (20), except that not all correlation terms evaluate to zero. Depending on the amount of correlation and which signals correlate, σ and σ represent some constant values that reflect the bundled correlation terms of equation (19).

$$\dots - \dots - \dots$$

Most notable about equation (21) is that the correlation terms are a proportional term applied to σ . That means that when one or more signals suffer from correlated noise, σ is expected to grow linearly with the number of samples. Note that σ is likely significantly larger than σ as the former represents e.g. σ and the latter represents e.g. σ which, in case σ and σ correlate is non-zero but clearly much smaller than the former. Furthermore, note that the σ term is scaled by σ and thus a larger position error is expected to increase the rate at which σ grows. As equation (21) again contains sums over N , σ will also be a stochastic variable.

3.1.5 Deterministic Noise & Communication Delay

A minor remark can be made regarding deterministic noise, or any non-constant trajectory of σ and σ for that matter. Namely, as already mentioned, it would be unwieldy to consider every possible trajectory, and it does not appear interesting to try to derive predictions for sets of trajectories that share certain traits. Therefore, this will be neglected.

Finally, communication delay can be accounted for. Recall equations (14.1 and 14.2). These show that when communication delay is considered, σ and σ always share the same time instance while σ never does. Therefore, it is reasonable to expect that σ is never correlated to σ or σ unless there is no delay. Mathematically, this appears to be the only effect communication delay may have on σ . Since the noise effects are sufficiently complex for this thesis, communication delay will not be investigated further in this thesis.

3.2 Magnitude of bookkeeping inaccuracy

The second research question asks which quantities affect the magnitude of bookkeeping inaccuracy. This question must be answered in two parts.

First, in the previous section, equations (20) and (21) were derived. These show which quantities affect the magnitude of the variance σ^2 as a stochastic variable. Furthermore, they show which quantities affect the growth of σ^2 in the case of correlated noise. The affecting quantities are position error, σ_p , the correlation terms represented by ρ , and the characteristics of the stochastic variables represented by σ_n , the MCI approximation error. This approximation error has characteristics that likely scale with the signal to noise (STN) ratio of the measurement signals σ_n/σ_p . The correlation terms scale with the amount of correlation between the noise on each measurement signal.

Secondly, so far, the behaviour of σ^2 has been predicted. But σ^2 being noise-sensitive does not strictly imply that the bookkeeping inaccuracy is impacted. To determine this, the behaviour of σ^2 must be compared to the noisy behaviour of the actual potential energy of the impedance controller. Specifically, for bookkeeping to be accurate, the level of the energy tank, which accumulates the observations of all energy observers, must be equal to the potential energy at all time instances. The potential energy is given in equation (22). It uses the same notation as used for equation (15).

$$\dots -$$

While the energy tank level is clearly dependent on all previous observations made by the energy observers, the potential energy, P , does not have such a dependency. It can always be known with only the controller state information of a specific time instance. It is immediately clear that if the measurement signals remain bounded, so does σ^2 .

It is possible to mathematically analyse equation (22) in the same way as was done for VIM, in an attempt to mathematically predict whether noise will induce a mismatch between σ^2 and the energy tank level. To make this prediction, a similar analysis must be performed for the work done observer. However, it was decided such an investigation is out of scope due to time constraints for this thesis. Instead, a possible mismatch between potential energy and the tank energy level will be investigated empirically through experiments.

3.3 Significance of Inaccuracy

The third research question asks at what order of magnitude the effects of noise on VIM will become noticeable in the functioning of the Two-Layer architecture. Specifically, when it will be noticeable in the transparency and passivity behaviour of the controller. If the behaviour of σ^2 dictates the behaviour of the energy tank level, then two predictions can be made.

First, in the correlated noise case, the energy tank level will always grow, linearly, even when the system is not operated or in motion. This will completely break any passivity guarantee, as the energy tank level can grow unbounded.

Secondly, in the uncorrelated noise case, the energy tank level will behave stochastically. This means that during or after a noisy operation, the energy tank may be left with residual energy or may run out of energy sooner, compared to the same operation without noise. This means that the controller is not passive, strictly speaking, in the case a residual energy remained. It also means the controller will hamper transparency sooner than it would have without noise, as the tank is drained sooner. Both of these effects should be noticeable by the operator.

So, in either case, it is expected that either the energy tank level will have some (growing) residual energy in it when it is not being operated, or that transparency is hampered more strongly than expected, which will be noticeable in the passivity limited control force. For inaccuracy to be significant, it could be stated that the passivity breaking effect is significant if it results in an energy tank trajectory similar to if the passivity controller was disabled, and the transparency hampering effect is significant if it results in a control force trajectory similar to that of trajectory without VIM.

This is an identifiable scenario and thus sufficient for a verifiable hypothesis.

3.4 Hypotheses

The derivation of the previous section led to the mathematical justification that only noise on the controller input signals affect the behaviour of VIM and through it the bookkeeping accuracy. Several circumstances and quantities were identified that influence the behaviour and magnitude of VIM. Based on these derivation results, a set of hypotheses will be posed that will be verified through experiments in the future sections.

The hypotheses are formulated in parallel to the research questions, such that when verified, they provide an insightful answer to each question.

3.4.1 Relevant realization factors

It was shown that noise causes the signals to be stochastic and this results in stochastic behaviour of VIM. Whether the stochastic signals correlate determines the exact stochastic prediction of this behaviour. Regardless, this stochastic behaviour of VIM is expected to cause the energy bookkeeping to deviate from the actual potential energy of the controller.

H1 - “ St o c h a s t i c n o i s e o n t h e c o n t r o l l e r i n p u t s i g n a l s w i l l a f f e c t t h e b e h a v i o u r o f V I M d i f f e r e n t l y t h a n i t w i l l a f f e c t t h e p o t e n t i a l e n e r g y . ”

3.4.2 Magnitude of bookkeeping inaccuracy

It was shown that the magnitude of stochastic variation of VIM and, in case of correlated noise, rate of growth of VIM are affected by a set of factors. It may be that the observed work done by the controller is affected in a similar way and thus the magnitude of VIM and the magnitude of the observed work done could be of similar order. However, if this is not the case, then it is expected that the factors that affect the magnitude or rate of VIM will also affect the bookkeeping inaccuracy. These factors are (1) the noise magnitude of the impedance and position signals; (2) the magnitude of the noise-free position error signal. These two factors will affect the magnitude of randomness of the VIM for both correlated and uncorrelated noise. In the case of correlated noise, the additional factor that influences the rate of growth of VIM is (3) correlation constant, in addition to the previous factors.

Bookkeeping inaccuracy is defined as the mismatch between the monitored energy, stored in the energy tank, and the actual potential energy of the impedance controller.

H2.1 - “The magnitude of the control input noise and the position error will affect the magnitude of bookkeeping inaccuracy.”

H2.2 - “In case the control input noise signals are correlated, VIM is expected to grow at a linear rate, unbounded, proportional to amount of correlation, position error, and noise magnitude.”

3.4.3 Significance of inaccuracy

If VIM dominates the energy tank behaviour, it is expected that VIM will induce either more energy storage in the energy tank than the controller has potential energy, or it will induce less energy storage in the tank than the controller has potential energy in which case it will activate passivity control.

Based on this, it is expected that when the magnitude of bookkeeping inaccuracy is significant, either (1) the energy tank will finish motions with a significant amount of positive energy in the energy tank while the system is at rest; Or (2) the control force will be set to 0 significantly sooner than it would have for the same motion performed with noise free signals, reducing transparency.

H3 - “ I f t h e m a g n i t u d e o f b o o k k e e p i n g a c c u r a c y i s s e e n t o b e s i g n i f i c a n t l y p o s i t i v e , t h e e n e r g y t a n k w h i l e t h e s y s t e m i s i n r e s t m a y g r o w s i g n i f i c a n t l y p o s i t i v e , o r t h e c o n t r o l f o r c e w i l l b e s e t t o z e r o b y t h e p a s s i v i t y c o n t r o l l e r s o o n e r t h a n i t w o u l d h a v e h a d t h e i n p u t s i g n a l s b e e n n o i s e f r e e . ”

Although this final hypothesis does not pose an exact answer to research question RQ3 in the form of an exact point of ‘significance’, it will provide a sufficient answer. Namely, to verify hypothesis H3, an approximate order of magnitude will be found at which the inaccuracy effects on passivity and transparency will and will not be distinguishable by observing the control force trajectory and the energy tank level. This demonstrates that noise can have significant effect and provides an idea for which rough circumstances and quantity values this effect may occur. This is more interesting than an exact point of significance, as it investigates the broader side of research question RQ3.

Chapter 4 Setup & Design

4.1 Materials

Both physical and simulation experiments will be conducted. The simulated experiments will be conducted in MATLAB and Simulink. The physical experiments will be conducted in a tele-operation setup facilitated by RAM in the IBotics lab. The relevant hardware available in the lab is the Myo armband, the Franka Emika Panda robotic arm, and the Omega X haptic device. The hardware will be integrated via the controller and the algorithm for this will be implemented via ROS [ROS, Franka, Omega].

ROS is an open-source framework that amongst other things aims to facilitate a general implementation of software that manages communication of data between different systems. It also allows for convenient community sharing of reusable code compatible with or aimed at ROS through packages. 'ROS control' and 'ROS Hardware' are such packages and provide a robot agnostic interface that can be used by robot developers to provide a standard interface for control programmers to conveniently implement control algorithms without worrying about the hardware implementation.

The Myo armband is a measurement device that performs Electro Myogram (EMG) measurements and sends these wirelessly to a processing device, such as the controller. Previous research at RAM yielded algorithms that process these raw EMG signals to provide normalized 'co-contraction' levels that represent tensing and untensing of the measured muscle according to calibration [8]. The muscle that will be measured for these experiments is the lower left arm. The Myo is a convenient out-of-the-package solution simplifying the process of measuring and processing EMG signals.

The Franka robot is a serial robot arm with 7 DoF. It is operated through a 'Franka ROS' package which provides a ROS control implementation that works with the 'Franka Hardware' package, an extension of ROS Hardware. The Franka ROS API comes with build in dynamic compensation and examples for implementing singularity (null space) avoidance and Coriolis compensation. It also provides the jacobian that can be used to convert a desired end-effector 'Wrench', a 6 DoF effort equivalent of force, to torques in the joint space. The Franka ROS package provides a set of example controller implementations in ROS which can be adapted. The 'Cartesian Impedance Controller' suits the needs for this thesis, only requiring the impedance control law to be replaced by a controller implementation suited for this thesis.

The Omega X is parallel robot arm able to detect 6 DoF displacement and apply a force. It is operated through a custom C++ API that allows reading the displacement measurements and setting a force to apply. The Omega requires a startup and shutdown procedure which was implemented in ROS code as a result of previous research work at RAM. The displacements are given as end-effector coordinates with respect to its home configuration. The application force is given with respect to its home configuration.

4.2 System Design & Implementation

As mentioned, the Omega X, Franka and Myo come with already existing code implementations that allow interfacing with the devices, such that only the controller needs to be implemented that integrates these interfaces into the control architecture.

The control architecture that will be used is as described in the background theory with some minor adjustments.

Namely, in the physical implementation, precaution will be taken to ensure safe operation for both the user and the durability of the robot. This is done by saturating the force within safe limits and limiting the force rate of change to avoid 'jitter', i.e. rapid on and off limiting of the control force. This

may affect the quality of the physical results as it hampers the effectiveness of passivity control, in which case this has to be kept in mind for future research.

Besides this, significant noise magnitudes with small to zero end-effector velocity, i.e. a bad STN ratio on the signals, will cause the sign of the predicted work done to be frequently predicted wrong. This makes the passivity algorithm significantly less effective in practice. However, in experience this is not an issue for relatively small noise magnitudes. Such small noise magnitudes are expected in the physical setup. However, in the simulation, noise will be increased to significantly large magnitudes for some experiments. Therefore, in simulation, the controller algorithm will not use a predictor as it was described in the background theory. Instead, it will use a noise-free position signal to predict the work done.

To validate the implementation, components such as VIM, jitter saturation, and the passivity controller can be enabled or disabled so that experiments can be conducted validating these features.

4.3 Experiment Design

The purpose of this section is to formulate a set of experiments that validate the baseline setup and verify the hypotheses. The goal of validation is to show that the baseline matches the state of the art of literature and goes no further than what has been explored in literature. This makes it likely that the consecutive results were obtained in a known environment where any new results are due to the purposeful adjustments to the setup. This provides for a valid investigation of the novel work of this thesis.

For each experiment, a set of variable 'flags' are either true or false. This represents components that are enabled, such as the passivity layer, or the addition of VIM to the energy tank. For the validation experiments these flags will logically be different. This will be clear in each subsection. In addition to the flags, several variables will be adjusted, set to be either constant or vary within a range. This will also be indicated per experiment.

For all experiments, the parameters in table 33-1 will remain constant. These parameters were chosen experimentally based on a trade-off between nominal values found in real setups, and value that expose the behaviour of the underlying processes so that the results will be meaningful.

There will also be some differences in settings between the physical and simulated setup. For the physical setup, some precautions are taken to promote safety. Namely, the impedance will range between lower levels and the passivity force will be saturated and rate limited to prevent dangerous forces as well as to prevent device wear and tear due to force jitter. Force jitter will occur due to passivity control. This will be demonstrated. In simulation, a perfect prediction of the future work done will be made. This prediction is a necessary part of the passivity controller, as described in the previous section. If the prediction is not perfect and the system suffers from large noise magnitudes, this affects the results and may break passivity depending on the algorithm. This will be demonstrated. Because this effect is not the focus of this thesis, it is justifiable to use a perfect predictor in the simulation.

Name	Value
Sample time (Omega & Myo)	0.01 seconds
Sample time (Franka)	0.001 seconds
Nominal position noise amplitude (simulation)	0.001 cm (0.0333% STN for constant 3 cm signal)
Nominal impedance noise amplitude (simulation)	12 N/m (2.4% STN for constant 500 N/m signal)
Significant position noise amplitude (simulation)	0.1 cm (3.33% STN for constant 3 cm signal)
Significant impedance noise amplitude (simulation)	60 N/m (12% STN for constant 500 N/m signal)
Force step rate limit (physical)	0.06 N (at sample time of 0.01 seconds)
Force saturation (physical)	15 N
Correlation of correlated signals	100% (the signals are constantly-scaled copies)

Table 33-1 – Table of parameters that remain constant across all experiments.

4.3.1 Validation

For each validation experiment, the parameters and variables in table 331-1 will remain constant. Table 331-2 provides the relevant information for each validation experiment.

The validation experiments will be conducted both in simulation and physically. The physical experiments are, however, harder to isolate from undesired effects such as noise and the control input trajectories are provided manually. This means the physical experiments will not be an exact replication of the simulated experiments.

Validation experiments 1 to 2 from table 331-2 are used to demonstrate that the passivity layer behaves as expected. That is, the passivity layer will ensure that the energy tank level will not become negative, meaning the system will never inject more energy into the environment than it absorbed.

Validation experiments 3 and 4 from table 331-2 are used to demonstrate that, with noise-free control input signals, adding VIM to the energy tank will ensure the energy bookkeeping is accurate even when the position error is non-zero during impedance modulation. This particular scenario is demonstrated, because it is expected in literature that without VIM the potential energy of the controller is changed in this scenario without this change being monitored by the passivity observer [8].

Name	Value
Simulation time	7 seconds
Local position trajectory	[0, 3] cm amplitude sine-based hills between time intervals [1, 3] and [4, 6] seconds.
Remote position trajectory	Constant at 0 cm.

Table 331-1 – Table of parameters that remain constant across validation experiments.

Nr.	Description	Passivity Layer	VIM	Impedance Trajectory
1	Demonstrate lack of passivity control	Off	Off	Start at 500 N/m, finish at 1000 N/m with a linear slope of [500, 1000] N/m at time interval [3.35 3.65] seconds.
2	Demonstrate effect of passivity control	On	Off	
3	Demonstrate lack of VIM when modulation occurs simultaneous to non-zero position error. Both a positive and negative slope for impedance is of interest	On	Off	Start at 500 N/m, finish at 500 N/m with a linear slope of [500, 1000] N/m at time interval [1.85, 2.15] seconds and a linear slope of [1000, 500] N/m at time interval [4.85, 6.7] seconds.
4	Demonstrate effect of VIM for the same scenario as experiment 3.	On	On	

Table 331-2 – Table of validation experiments

4.3.2 Relevant realization factors

To verify hypothesis H1, validation experiment 4 from table 331-2 can be repeated. However, now with varying noise magnitude. Table 332-1 provides the details of parameters and variables that remain constant. Table 332-2 provides the experiment details.

Varying noise magnitude can only be done in simulation, as the facilities and time lack to create a physical setup to control noise. Therefore, the verification experiments of table 332-2 will only be done in simulation. The noise is either nominal or significant. Nominal noise is of a magnitude similar to the noise on the signals of the physical setup. All noise will be white noise generated via MATLAB's "rand()" function.

The verification experiments of table 332-2 will verify the hypothesis H1 because they allow demonstrating the difference between the energy tank levels and the actual potential energy of the controller.

Name	Value
Simulation time	7 seconds
Local position trajectory	[0, 3] cm amplitude sine-based hills between time intervals [1, 3] and [4, 6] seconds.
Remote position trajectory	Constant at 0 cm.
Impedance trajectory	Start at 500 N/m, finish at 500 N/m with a linear slope of [500, 1000] N/m at time interval [1.85, 2.15] seconds and a linear slope of [1000, 500] N/m at time interval [4.85, 6.7] seconds.

Table 332-1 – Table of parameters that remain constant across H1-verification experiments.

Nr.	Description	Noise
1	Demonstrate the effect of nominal noise on VIM.	Nominal
2	Demonstrate the effect of significant noise on VIM.	Significant

Table 332-2 – Table of H1-verification experiments

4.3.3 Magnitude of bookkeeping inaccuracy

To verify hypothesis H2.1, the noise magnitude will be varied for a constant position error and vice versa. To verify hypothesis H2.2, only the noise magnitude will be varied, for a non-zero constant position error. The noise will be correlated noise. The proportionality to sample time and position error will not be investigated, as this will make the analysis and experiment design too complex for what it is worth. Instead, the prediction made in the derivation section, equation (eq21), will be compared to the observed VIM contribution to the energy tank. Table 333-1 provides the details of parameters and variables that remain constant. Table 333-2 provides the experiment details. For the same reasons as in the previous subsection, the experiments will only be conducted in simulation.

The verification experiments of table 333-2 will verify the hypothesis H2.1 because they allow demonstrating that the difference between the energy tank levels and the actual potential energy of the controller will change with the varying noise magnitude and varying position error. For hypothesis H2.2, it allows demonstrating that correlated noise causes an unbounded contribution by VIM.

Name	Value
Simulation time	7 seconds
Remote position trajectory	Constant at 0 cm.
Impedance trajectory	Constant at 500 N/m

Table 333-1 – Table of parameters that remain constant across H2-verification experiments.

Nr.	Description	Noise	Position error
1	Demonstrate the effect of no noise on VIM.	None	3 cm
2	Demonstrate the effect of nominal noise on VIM.	Nominal	3 cm
3	Demonstrate the effect of significant noise on VIM.	Significant	3 cm
4	Demonstrate the effect of position error on VIM	Significant	0 cm
5	Demonstrate the effect of position error on VIM	Significant	1.5 cm
6	Demonstrate the effect of position error on VIM	Significant	3 cm
7	Demonstrate the effect of correlated noise on VIM	None	3 cm
8	Demonstrate the effect of correlated noise on VIM	Nominal	3 cm
9	Demonstrate the effect of correlated noise on VIM	Significant	3 cm

Table 333-2 – Table of H2-verification experiments

4.3.4 Significance of inaccuracy

To verify hypothesis H3, no additional experiments need to be conducted. Instead, the experiments of table 332-2 will be sufficient. Namely, these demonstrate the effect of VIM given nominal to significant noise in simulation. To then verify the hypothesis, the effect of VIM on the control force and the energy tank trajectories in these experiments must be observed and compared with the noise-free scenario of validation experiment 4 of table 331-2.

Chapter 5 Results

5.1 Validation

The results of the validation experiments will be demonstrated in this section. It is subdivided into several subsections. Namely, results regarding the validation of the passivity layer; of the VIM technique; and a brief demonstration of the nominal noise of the physical setup for a static system with constant inputs. Each subsection first addresses the simulation results, where applicable, and then the corresponding physical results.

5.1.1 Validation – Passivity Layer

The results of validation experiments 1 and 2 of table 331-2 are illustrated in figure F411-1 for simulation, and figure F411-2 for physical experiments. The true potential energy of the controller is computed offline based on the control input signals and compared with the energy tank. In simulation it is visible that the potential energy with passivity off does not match the monitored energy. The monitored energy goes below zero. Furthermore, when passivity action occurs causing the control force to be set to zero, this also causes a mismatch between the monitored energy and the potential energy.

In the physical experiments, these observations can be recognized in the data as well. Specifically, with passivity off, the monitored energy is a stronger mismatch to the potential energy, lying significantly further beneath zero, than with passivity on. With passivity on, however, the monitored energy still becomes negative. Crossing the energy tank zero line corresponds simultaneously with the rate-limited passivity action. Due to the rate-limit, the passivity controller cannot set the control force to zero in one time step.

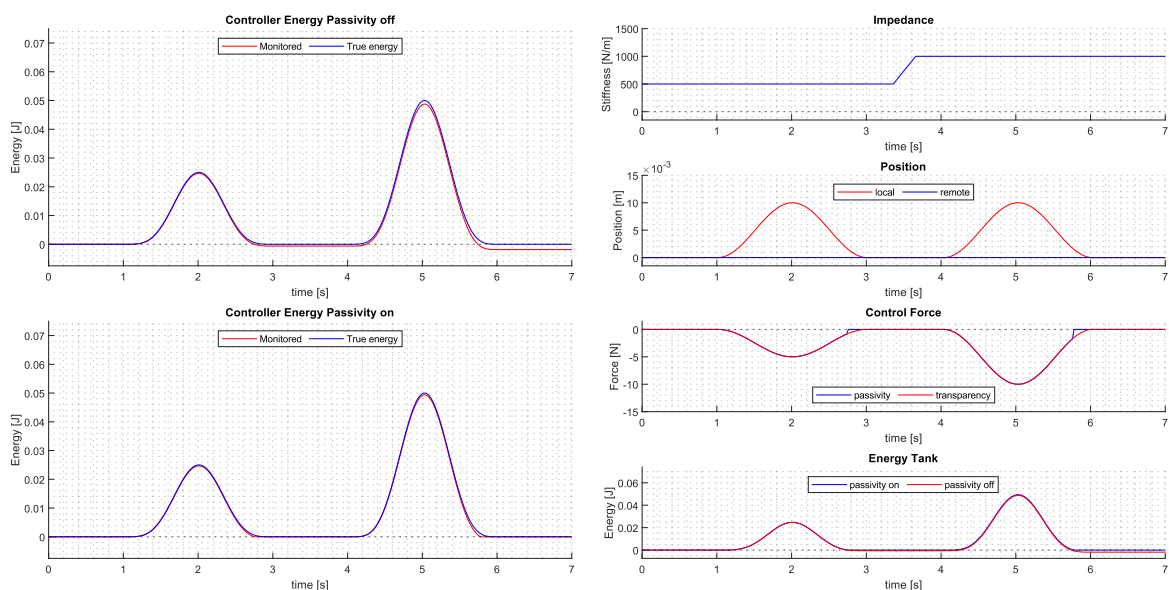


Figure F411-1 – The top and bottom left graphs plot the ‘monitored’ energy tank levels and the ‘true’ potential energy of the controller. The right graphs, top to bottom, plot the impedance, position, control forces, and energy tank trajectory. For the control force, both the passivity and transparency forces are shown for ‘passivity on’ only, as the transparency forces for both ‘on’ and ‘off’ scenarios are identical. For the energy tank, both ‘passivity on’ and ‘off’ are shown.

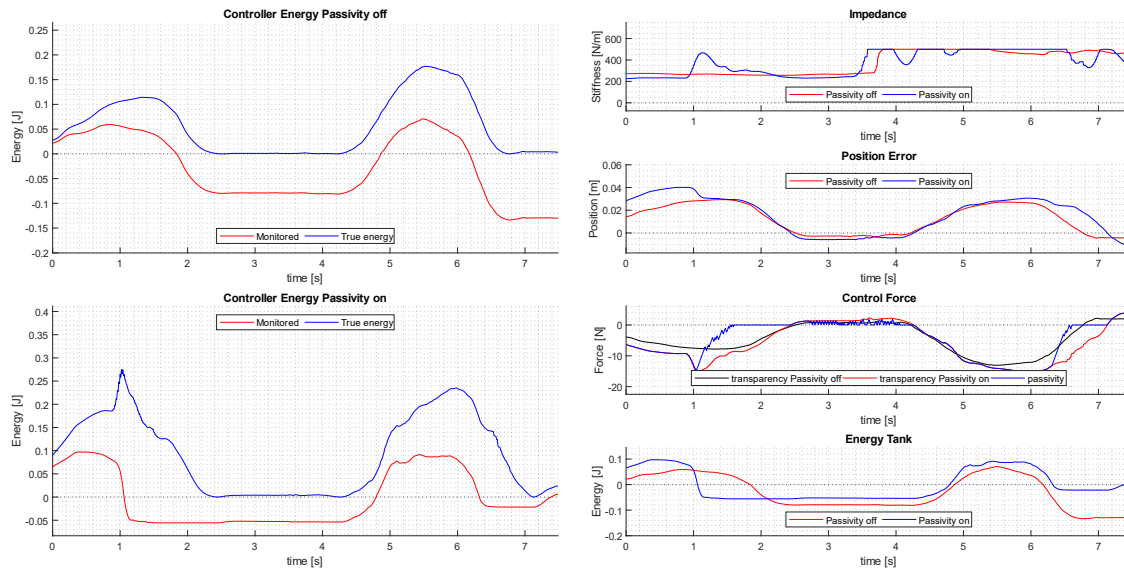


Figure F411-2 – The top and bottom left graphs plot the ‘monitored’ energy tank levels and the ‘true’ potential energy of the controller. The right graphs, top to bottom, plot the impedance, position, control forces, and energy tank trajectory. Because the input trajectories, i.e. impedance and position error, could not be perfectly reproduced, both measurements during the ‘passivity off’ and ‘on’ scenario are plotted. All data was time-shifted such that the two position measurements approximately lined up. For the control force, both the passivity and transparency forces are shown for ‘passivity on’, while only transparency is shown for ‘passivity off’. For the energy tank, both ‘passivity on’ and ‘off’ are shown.

5.1.2 Validation - VIM

The results of validation experiments 3 and 4 of table 331-2 are illustrated in figure F412-1. The monitored energy with VIM off is a clear mismatch with the potential energy of the controller. With VIM on there is once again minimal mismatch, comparable to the situation of passivity on of figure F411-1.

Results of the physical experiments are illustrated in figure F412-2. There is a clear mismatch, regardless of whether VIM is on or off. However, with VIM on, the details in the ‘monitored’ energy curve clearly represent the details of the potential energy curve. Notable for the VIM on scenario is that the mismatch starts to occur when the control force reaches the saturation point of 15N as well as when the passivity controller limits the control force due to the energy tank reaching zero. Outside of these moments, the curves appear to align.

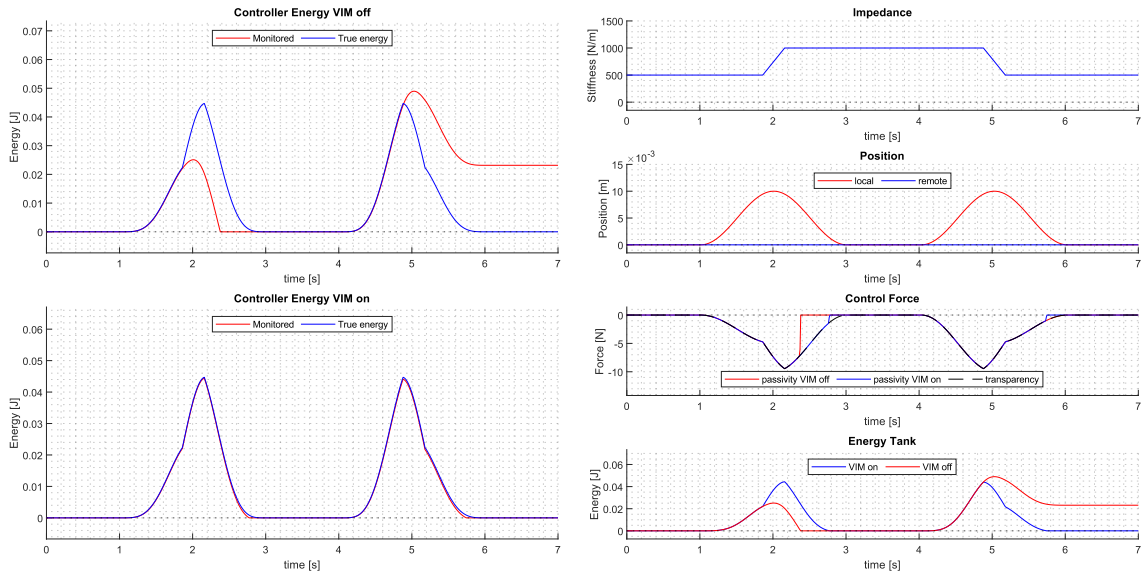


Figure F412-1 – The top and bottom left graphs plot the ‘monitored’ energy tank levels and the ‘true’ potential energy of the controller. The right graphs, top to bottom, plot the impedance, position, control forces, and energy tank trajectory. For the control force, both the passivity for ‘VIM on’ and ‘off’, and transparency forces are shown. The transparency forces are identical for both scenarios. For the energy tank, both ‘VIM on’ and ‘off’ are shown.

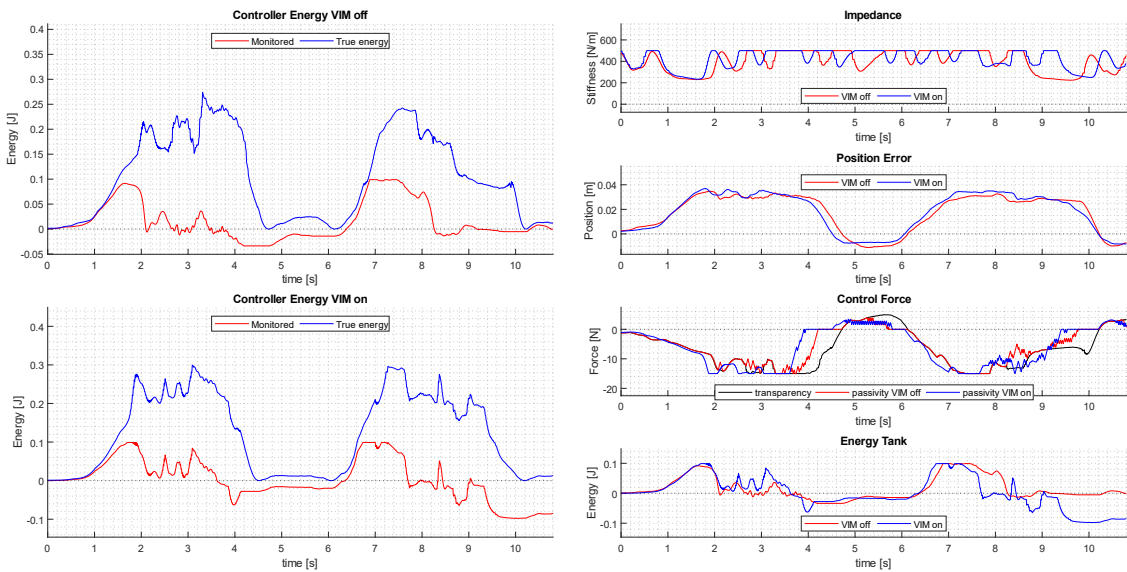


Figure F412-2 – The top and bottom left graphs plot the ‘monitored’ energy tank levels and the ‘true’ potential energy of the controller. The right graphs, top to bottom, plot the impedance, position, control forces, and energy tank trajectory. Because the input trajectories, i.e. impedance and position error, could not be perfectly reproduced, both measurements during the ‘VIM off’ and ‘on’ scenario are plotted. All data was time-shifted such that the two position measurements approximately lined up. For the control force, both the passivity and transparency forces are shown for ‘VIM on’, while only transparency is shown for ‘VIM off’. For the energy tank, both ‘VIM on’ and ‘off’ are shown. The control force is saturated at 15N.

5.1.3 Static Nominal Noise

In figure F413-1 the measurement results are illustrated for each system device. In table T413-1, the variance and difference between minimum and maximum of each complete signal is given.

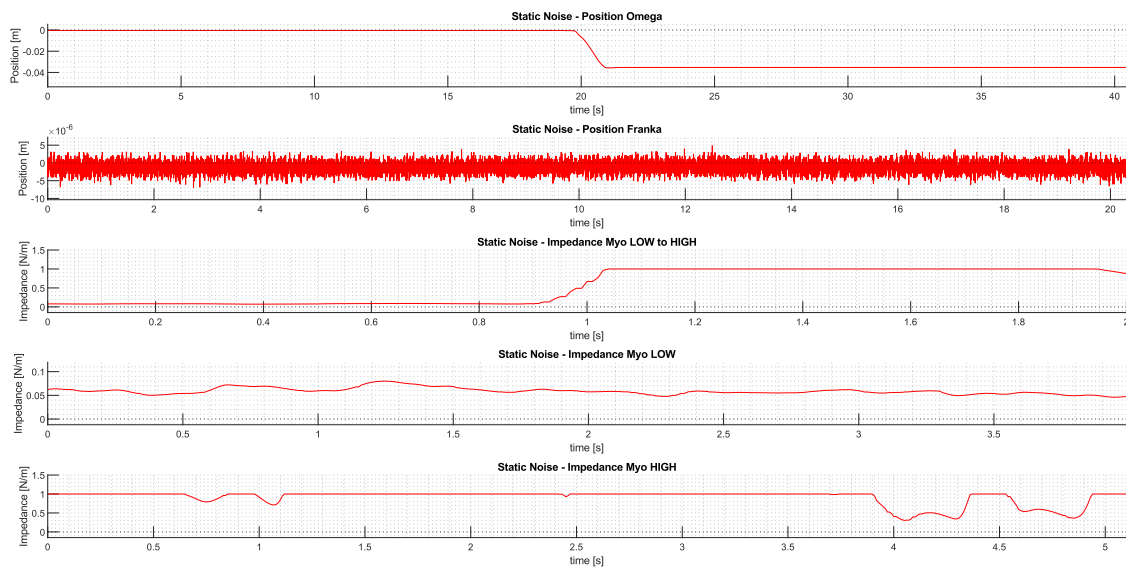


Figure F413-1 Measurements of the Omega, Franka, and Myo, disconnected from each other. The devices receive a constant input. For the 1st signal from the top, the operator changes the Omega position to a different constant input. For the 3rd signal from the top, the operator tenses her arm muscle and thus the Myo measurement to a different constant input. The Omega signal appears filtered by the omega device before being read-out. The Franka signal is not filtered. The Myo co-contraction signal appears to saturate at the ‘HIGH’ level, suppressing some of the noise.

Plot number - Signal	Variance	Min-max difference
1 - Omega	-	-
2 - Franka	0.0001437 cm	0.001175 cm
3 - Myo Low to High	-	-
4 - Myo Low	$0.007 \times 500 \text{ N/m} = 3.5 \text{ N/m}$	$0.034 \times 500 \text{ N/m} = 17 \text{ N/m}$
5 - Myo High	-	-

Table T413-1 – Table displaying the variance and min-max difference of each signal. The values were computed in MATLAB using “ $\text{sqrt}(\text{var}(x))$ ” for the variance and “ $\text{max}(x)-\text{min}(x)$ ” for the min-max difference. The min-max difference results are comparable to the nominal noise amplitudes used in simulation. For plots 1, 2, and 3, the variance and min-max difference were not applicable as the Omega signal is filtered, and when the Myo signal is ‘HIGH’ the signal is saturated, making these signals unsuitable for noise analysis. Note that the Myo signal represents the co-contraction levels. These were converted to an impedance value by multiplying by 500 N/m so that maximal co-contraction corresponds to an impedance increase of 500 N/m which matches the maximal impedance change in simulation.

5.2 Verification - Relevant realization factors

The results of verification experiments 1 and 2 of table 332-2 are illustrates in figure F42-1 together with the result of experiment 4 of table 331-2. The trajectories with nominal noise, do not appear any different from the noise-free trajectories. However, the trajectories with significant noise do appear different. The control force is set to 0 sooner than for the trajectories with less noise magnitude. The

monitored energy does not match the potential energy of the controller. The final energy tank level after the motion is negative.

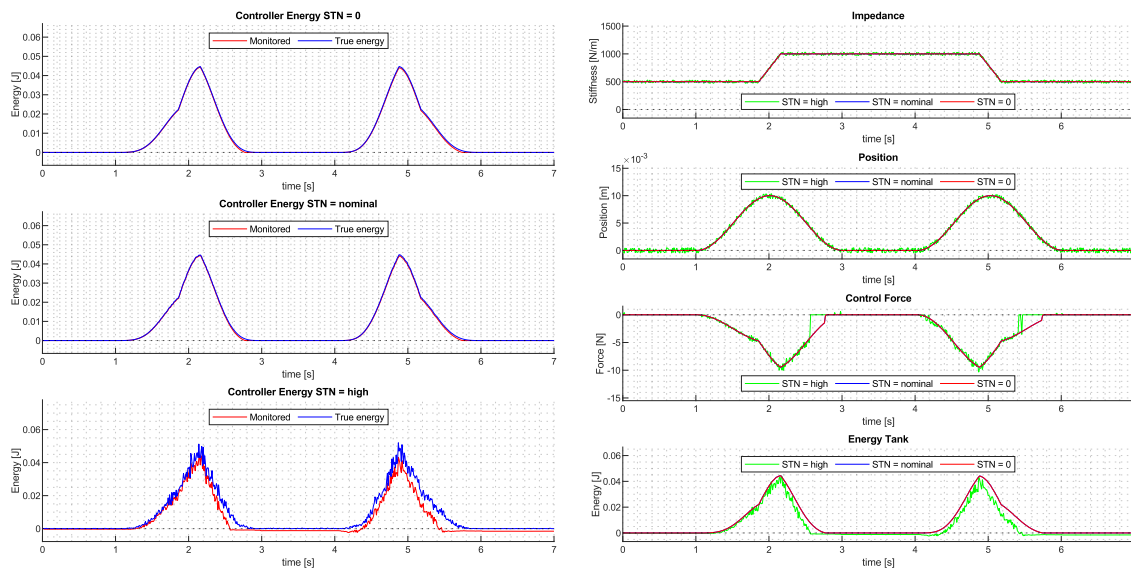


Figure F42-1 – The top to bottom left graphs plot the ‘monitored’ energy tank levels and the ‘true’ potential energy of the controller for different noise magnitudes (signal to noise (STN) ratios). The right graphs, top to bottom, plot the impedance, position, control forces, and energy tank trajectory. For the control force, the passivity forces are shown for different noise magnitudes. For the energy tank, the levels are shown for different noise magnitudes.

5.3 Verification - Magnitude of bookkeeping inaccuracy

Not all results of verification experiments 1 to 9 of table 333-2 are illustrated as figures, but instead given in tables. Due to randomness potentially skewing the results, the experiments were ran 100 times. The mean of the difference between monitored and potential energy is taken. These results are given in table T43-1. In the table, it is noticeable that large noise magnitude and larger position error results in a greater mean mismatch. Furthermore, correlation in noise results in a mismatch several factors larger for nominal noise compared to uncorrelated noise. However, for significant noise, both correlated and uncorrelated noise cause a mismatch of similar magnitude.

Figure F43-1 illustrates the experiments 7 to 9 for correlated noise. The other experiments yielded similar results, hence the table provides more insight. Figure F43-2 illustrates the accumulated energy monitored by each energy observer separately. For the VIM observer, the predicted energy trajectory, derived in ‘Chapter 3 Analysis’ in ‘Section 3.1.2 Stochastic Noise’, is plotted alongside the data. Both the complete prediction given by equation (19) and the truncated prediction of , which does not include any covariances of 3 signals, are plotted. The truncated prediction appears to be a better fit.

Experiment	Mean energy mismatch	Standard deviation	Noise magnitude	Position Error	Correlated
1	0	0	Zero	3 cm	No
2	-3.28	1.6	Nominal	3 cm	No
3	-1.9	1.2	Significant	3 cm	No
4	-1.37	8.5	Significant	0 cm	No
5	-6.6	0.4	Significant	1.5 cm	No
6	-1.9	1.2	Significant	3 cm	No
7	0	0	Zero	3 cm	Yes
8	-2.2	1.6	Nominal	3 cm	Yes
9	-1.5	1.3	Significant	3 cm	Yes

Table T43-1 – Mean and standard deviation of the monitored vs actual potential energy mismatch, per experiment. Each experiment was ran 100 times. The experiment number refers to the experiment of table 333-2.

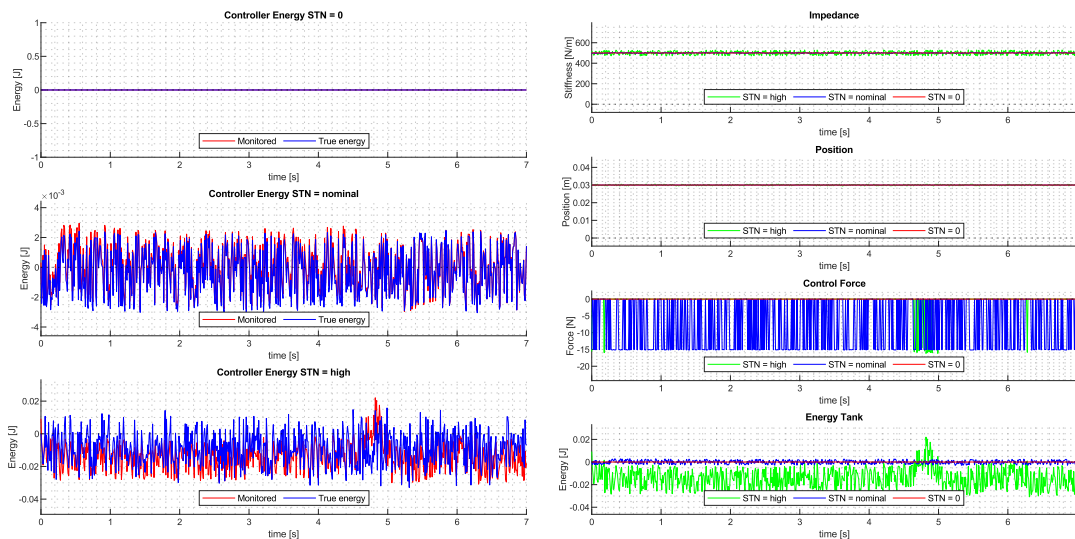


Figure F43-1 – The top to bottom left graphs plot the ‘monitored’ energy tank levels and the ‘true’ potential energy of the controller for different noise magnitudes (signal to noise (STN) ratios). The right graphs, top to bottom, plot the impedance, position, control forces, and energy tank trajectory. For the control force, the passivity forces are shown for different noise magnitudes. For the energy tank, the levels are shown for different noise magnitudes.

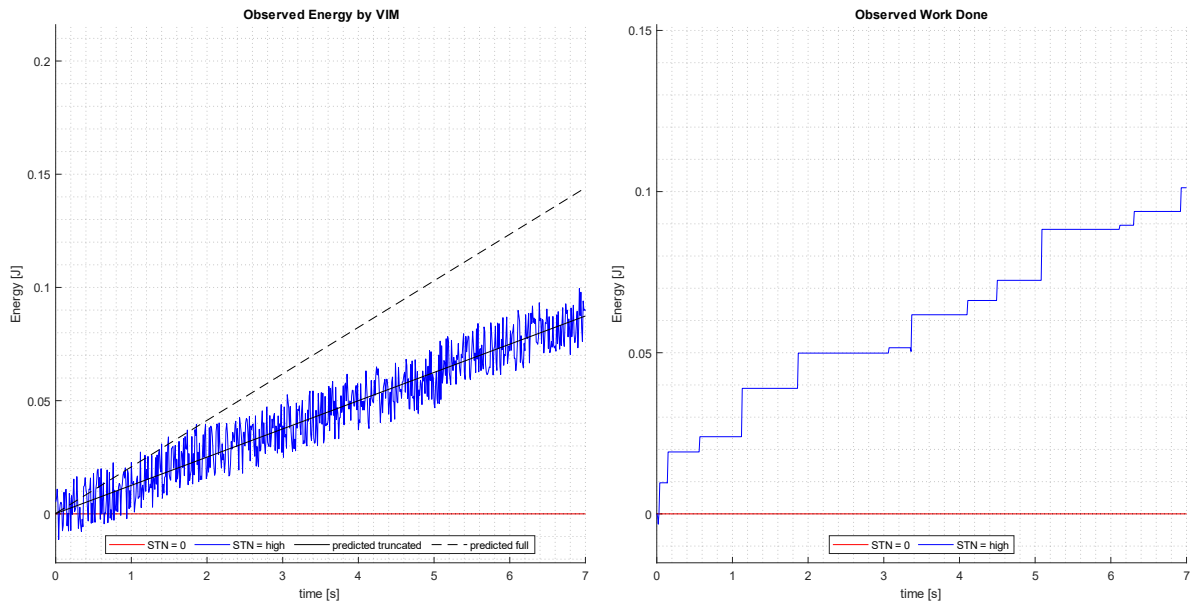


Figure F43-2 – Contributions of energy to the energy tank by each energy observer. Left shows the energy contribution by the VIM observer, right by the work done observer. In the left plot, the truncated prediction and full prediction are plotted, respectively as a unbroken and dashed line.

Chapter 6 Discussion

In this chapter, the results of the previous chapter will be discussed. This is done in the order of validation followed by the verification of each hypothesis. In each section, first any expected results will be discussed. Then, issues and deviations of the hypotheses and expectations. Finally, possible causes or explanations of these issues and deviations will be mentioned.

6.1 – Validation

6.1.1 – Simulation

Figures F411-1 and F412-1 mostly show results in line with what was found previously in literature. What was investigated in literature previously is shown in the right set of graphs in each figure. Specifically, the energy tank and control force trajectories show that passivity is broken without the passivity layer; that transparency is reduced without VIM while modulating impedance while the energy tank ends up with residual energy after a motion; and that including VIM reduces the transparency hampering and appears to improve the energy tank trajectory.

What has not been done in literature is to compare the monitored energy, with the addition of VIM, to the actual potential energy of the impedance controller. This comparison is displayed in the left set of graphs in each figure. First of all, this comparison provides the additional insight that a lack of VIM causes a significant mismatch between the monitored energy and potential energy, from now on referred to as energy mismatch. This energy mismatch is remedied almost completely by including VIM in the energy tank update rule.

Despite VIM, however, even without noise, there is a very slight energy mismatch visible. This mismatch starts well before the passivity controller start to limit the desired force. This suggests VIM may not be an entirely accurate representation of the potential energy change due to impedance modulation.

6.1.2 – Physical

The physical results shown in figures F411-2 and F412-2 show that part of the implementation of the algorithms was likely flawed. Namely, the force rate limiting and force saturation appear to have caused a greater energy mismatch. This can be concluded as a strong energy mismatch appears to occur whenever the force gets saturated and whenever the passivity controller limits the force but cannot fully limit it due to the rate limit imposed on the force.

Another flaw in the physical experiments was due to the Omega and Myo being difficult to operate, making a perfect replication of the simulation input trajectories difficult. In particular, the Myo algorithm sometimes had difficulty to properly calibrate and thus did not accurately represent the muscle tensions of the operator. Furthermore, for the Omega, whenever transparency is reduced, this is noticeable for the operator, and this was experienced to negatively impact the operator's ability to not deviate off the desired trajectory.

6.1.3 – Noise analysis

The noise analysis was done to demonstrate that indeed the simulated nominal noise represents nominal circumstances on state-of-the-art robotics measurement devices. The simulation settings were, of course, based on these findings.

It was hard to avoid the build-in filtering in the Omega and Myo signals within a reasonable timeframe. This filtering may have affected the physical results as well. However, not significantly so, as some randomness still occurred in the Myo signal, and the unfiltered Franka signal added sufficient randomness to the position error signal.

6.2 – Relevant Realization Factors

The first hypothesis was: **H1 - “ Stochastic noise on t affect bookkeep- r o l l e r i n g a c c u r a c y b y a f f e c t i n g t h e b e h a v i o u r o f V I M d**

From figure F42-1 It is clear that noise affects the accuracy of bookkeeping, verifying the hypothesis. Specifically, noise affects both the potential energy and the monitored energy. However, it does so differently, resulting in a mismatch and thus a bookkeeping inaccuracy.

From the derivation, specifically equation (16), it was expected that noise accumulates randomly through VIM as the energy tank level is dependent on the past values of VIM. From the potential energy equation, it is clear that the potential energy of the impedance controller does not depend on the past, but only on the current states of the controller. Therefore, this result is as expected.

6.3 – Magnitude of bookkeeping accuracy

The second hypothesis consisted of a pair of sub-hypotheses. The first sub-hypothesis was: **H2.1 - “ T h e m a g n i t u d e o f t h e c o n t r o l i n p u t n o i s e a n d t h e p o s i t i o n e r r o r w i l l a f f e c t t h e m a g n i t u d e o f b o o k k e e p i n g i n a c c u r a c y . ”**

Figure F43-1 and table T43-1 show a random energy tank signal. Clearly both noise magnitude (indicated as STN) and position error affect the magnitude of variance of this signal. It is also clear there is an energy mismatch and the average mismatch between the monitored and actual potential energy increases with an increase of noise magnitude and position error as well. This verifies the hypothesis.

The second sub-hypothesis was: **H2.2 - “ I n c a s e t h e c o n t r o l i n p u t n o i s e e x p e c t e d t o g r o w a t a l i n e a r r a t e , u n b o u n d e d , p r o p o r t i o n a l t o t h e s a m p l e t i m e , a m o u n t o f c o r r e l a t i o n , a n d p o s i t i o n e r r o r . ”**

Table T43-1 demonstrates that whether the noise on the signals is correlated has no noticeable effect on the energy tank level. However, correlation does significantly change the behaviour of the VIM energy observer and the work done observer. This is visible in figure F43-2. In this, the truncated prediction accurately predicts the behaviour of VIM. While the full prediction appears to overestimate the VIM behaviour. It is not clear why the full prediction is not as accurate. Perhaps an incorrect assumption was made in the background regarding the covariance in equation (12). Regardless, the match between the behaviour of VIM with correlated noise signals, and the predicted trajectory, verifies the hypothesis.

As a side note, it was not expected that the observed work done would also grow unbounded due to noise. Since the observed work done grows at the same rate as VIM, the energy observers completely compensate each other's growth, leaving only some random, seemingly bounded difference. Another interesting insight is that, regardless of correlation, the work done observer is affected by noise. As far as this author is aware, this was not readily remarked in literature. The behaviour of the work done observer was not analysed, therefore no further remarks will be made as to why noise affects it.

6.4 – Significance of inaccuracy

The third and final hypothesis was: **H3 - “ I f t h e m a g n i t u d e o f b o o k k e e p i n g a m o u n t o f r e s i d u a l e n e r g y i n t h e e n e r g y t a n k w h i l e t h e s y s t e m i s i n r e s t m a y g r o w s i g n i f i c a n t l y p o s i t i v e , o r t h e c o n t r o l f o r c e w i l l b e s e t t o z e r o b y t h e p a s s i v i t y c o n t r o l l e r s o o n e r t h a n i t w o u l d h a v e h a d t h e i n p u t s i g n a l s b e e n n o i s e f r e e . ”**

From figure F42-1, it is clear that for a typical set of input trajectories, large noise magnitude causes significant inaccuracy. It is determined to be significant as this inaccuracy noticeably affects the

transparency of the system by invoking force limiting action by the passivity controller significantly sooner than would happen without noise. This verifies the hypothesis.

For nominal noise magnitudes, the effect of noise is not noticeable, and the trajectories appear to closely match the noise-free scenario. The large noise magnitude on the position that was considered is about a factor 100 larger than seen for Franka position measurements.

As a side note, figure F43-2 also demonstrates additional insights in regard to significance of inaccuracy. Namely, both energy observers observe an unbounded amount of energy flow over the power ports they monitor, even when this observation is clearly inaccurate, i.e. for constant inputs. This means that if there is a case where the work done observer does not, incorrectly, subtract as much energy as VIM, incorrectly, adds to the energy tank, the energy tank may fill or drain to an unbounded and possibly unpredictable level. It is not certain whether work done will always compensate VIM, meaning that in the presence of noise, passivity can simply no longer be guaranteed without additional proof. This suggests the effect of noise may be more significant than initially expected in this thesis.

Chapter 7 Conclusion

This thesis aimed to investigate the behaviour of VIM and the resulting bookkeeping accuracy for systems suffering from noise. Current literature has yet to investigate or prove the effects noise has on VIM and physical demonstration as well as thorough experimental investigation has been lacking. This thesis set three research questions to achieve this goal. The answers and related findings to each of these questions will be presented in this chapter. After that, limitations of the research of this thesis will be addressed and the consequences of the findings will be pointed out. A scope will be provided for future research that may logically follow from this. Finally, this thesis will be concluded.

7.1 – Relevant Realization Factors

RQ1 - “ Which realization factors affect bookkeeping i n g ? ”

The answer to RQ1 is that noise can cause bookkeeping to be inaccurate, which was demonstrated by comparing the monitored energy, i.e. the energy tank level, with the actual potential energy of the impedance controller based on its states. Combining the results of the noise-free simulated validation experiments with the observation that noise induces a mismatch in monitored and potential energy, it is clear that something is missing in the derivation of VIM or possibly the general incorporation of energy observers in TDPC when significant noise is involved. The energy tank level being dependent on past observations of the energy observers, which may be noisy, may be the cause of the mismatch with the potential energy, which is not dependent on the past.

7.2 - Magnitude of bookkeeping accuracy

RQ2 - “ Which circumstances or quantities affect the presence of inaccuracy inducing realization fact

The answer to RQ2 is that noise magnitude position error, and correlation affect the behaviour and magnitude of VIM. Specifically, noise magnitude and position error affect mean of the energy tank randomness as well as the variance of the randomness. Noise correlation between signals does not appear to affect the energy tank directly, but does appear to affect the behaviour of VIM, causing it to observe an unboundedly growing energy flow. The rate of growth is predictable and linear.

7.3 - Significance of inaccuracy

RQ3 - “ What order of magni ~~affecting quantities have fore~~ bookkeeping c u r a c y inaccuracy to have significantly noticeable effects on transparency or p a s s i v i t y ? ”

The answer to RQ3 is that significant noise has significant effect on the transparency and passivity of the control algorithm. Specifically, significant noise causes inaccuracy in energy bookkeeping. This in turn hampers transparency noticeably. It may also bring the energy tank level to below zero. As bookkeeping inaccuracy means that monitoring cannot be relied upon anymore, it is not clear whether an energy tank level less than zero indicates passivity was strictly broken, or merely incorrectly observed to be broken. Either way, under influence of significant noise, passivity can no longer be guaranteed through the Two-Layer architecture or TDPC until proven otherwise.

7.4 – Limitations & Improvements

There were several shortcomings in the execution of the physical experiments, both due to difficulty of operation and the implementation of various algorithms. The physical experiments, however, were intended as supportive evidence to the main evidence, which was gathered through more reliable simulation experiments. Therefore, the conclusions drawn for this thesis are unlikely to change due to improvements in the physical experiments. However, a deeper understanding may still be obtained

through such experiments. In improving the physical setup, it is recommended to (1) make operation easier; (2) remedy the implementation issues, primarily by improving the EMG calibration algorithm, avoiding force saturation or accounting for it in the observer, and remedying jitter in a different way than force rate limitation; (3) build a setup that allows signal noise to be controlled, e.g. by switching out different quality sensors.

7.5 – Consequences

To nuance the conclusions so far, noise is something that can be dealt with in various ways, including filtering as well as designing sufficient estimators and predictors. Whether noise forms a limitation in applying VIM depends on the design of these estimators and predictors, as well as on application requirements. It is imaginable that applications with high precision requirements are more likely to suffer from bad signal to noise ratios and thus may suffer from the noise sensitivity of VIM and possibly energy observers in general.

The fact that noise can induce bookkeeping inaccuracy through VIM exposes that a wrong assumption is made somewhere in either the derivation of VIM or the use of energy observers in TDPC. Before the cause of this inaccuracy is identified and remedied, it may be wondered to what extent system designers may rely on energy bookkeeping and TDPC.

An unexpected insight from the experiments was that correlated noise induces unbounded growth of the accumulated, observed energy in both the VIM and work done observers. In the correlation experiment that was performed, the two observers mostly cancelled out each other's observations. However, unless investigated further, there is no reason to expect that this cancelling always occurs. This means that passivity is no longer generally guaranteed, and transparency can be significantly hampered in certain scenarios. This effect may not be inherent to VIM, but instead be tied to the ability of virtual power ports to add an unconstrained amount of energy to the energy tank. Authors have investigated this effect in the past, as was briefly mentioned in the related work, and found it warranted to constrain such virtual power ports [3, 7]. This thesis has demonstrated additional scenarios in which this is important.

7.6 – Future Research

Identifying and remedying the demonstrated bookkeeping inaccuracies that occur even when no noise is present may be an important next step in enabling high-performance modulated-tele-impedance in practical settings. It may also be considered absolute necessity before deploying VIM in application areas where even the slightest of errors can have grave risks, such as in robotic surgery.

Asides from this, research in the behaviour of VIM and resulting bookkeeping accuracy under nominal noise circumstances seems to be almost concluded with this thesis. What remains is to conduct clean physical experiments according to the recommendations prescribed earlier.

7.7 – Conclusion

Despite literature having suggested that VIM ensures exactly accurate energy bookkeeping for modulated-impedance control, under simulated circumstances where noise of significant magnitude is present, energy bookkeeping is no longer accurate. Even when a system is noise-free, there appears to be a slight bookkeeping inaccuracy.

However, this noise-free inaccuracy appears negligible in simulation, and nominal circumstances involve a noise magnitude that is a few orders of magnitude below the significant magnitude. Therefore, while overly noisy or high precision applications may find VIM alone insufficient without precautions, applications experiencing nominal noise will find VIM satisfactory.

Bibliography

- [1] "Bilateral Telemanipulation With Time Delays: A Two-Layer Approach Combining Passivity and Transparency", Michel Franken et al.
- [2] "Geometric Grasping and Telemanipulation", C. Secchi et al.
- [3] "A Tank-Based Approach to Impedance Control with Variable Stiffness", Federica Ferraguti et al.
- [4] Yoon Sang Kim and B. Hannaford, "Some practical issues in time domain passivity control of haptic interfaces,"
- [5] "Friction Compensation in Energy-Based Bilateral Telemanipulation", Franken et al.
- [6] "Passive Hierarchical Impedance Control Via Energy Tanks", Alexander Dietrich et al.
- [7] "An Energy Tank-Based Interactive Control Architecture for Autonomous and Teleoperated Robotic Surgery", Federica Ferraguti et al.
- [8] "Intuitive Impedance Modulation in Haptic Control using Electromyography", MSc. Thesis by Kees van Teeffelen.
- [9] "A comprehensive review of haptic feedback in minimally invasive robotic liver surgery: Advancements and challenges", Mostafa Selim et al.
- [10] You, K., Zhou, C., & Ding, L. (2023). Deep learning technology for construction machinery and robotics. *Automation in Construction*, 150, 104852. <https://doi.org/10.1016/j.autcon.2023.104852>
- [11] Moniruzzaman, M., Rassau, A., Chai, D., & Islam, S. M. S. (2022). Teleoperation methods and enhancement techniques for mobile robots: A comprehensive survey. *Robotics and Autonomous Systems*, 150, 103973. <https://doi.org/10.1016/j.robot.2021.103973>
- [12] J. Buchli, E. Theodorou, F. Stulp, S. Schaal. "Variable Impedance Control: A Reinforcement Learning Approach" in Proc. of Robotics: Science and Systems, Zaragoza, Spain, Jun. 2010
- [14] Hokayem, P. F., & Spong, M. W. (2006). Bilateral teleoperation: An historical survey. *Automatica*, 42(12), 2035-2057. <https://doi.org/10.1016/j.automatica.2006.06.027>
- [15] "Mathematical Control Theory I", M. Kanat Camlibel et al., chapter 3
- [16] Assumed commonly available knowledge that does not require citing? (e.g. the laws have a Wikipedia page)
- [17] ROS Website (27 September 2024) www.ros.org
- [18] Franka github (27 September 2024) https://frankaemika.github.io/docs/franka_ros.html
- [19] Omega documentation (27 September 2024) www.forcedimension.com